Physics Faculty Research & Creative Works

Physics

01 Aug 2023

Doubly Differential Ionization In Proton-helium Collisions At Intermediate Energies: Energy Distribution Of Emitted Electrons As A Function Of Scattered-projectile Angle

K. H. Spicer

C. T. Plowman

Michael Schulz
Missouri University of Science and Technology, schulz@mst.edu

A. S. Kadyrov

Recommended Citation

Doubly differential ionization in proton-helium collisions at intermediate energies: Energy distribution of emitted electrons as a function of scattered-projectile angle

K. H. Spicer [1,*] C. T. Plowman [1], M. Schulz,[2] and A. S. Kadyrov [1,3]

[1]*Department of Physics and Astronomy, Curtin University, GPO Box U1987, Perth, WA 6845, Australia*
[2]*Physics Department and LAMOR, Missouri University of Science & Technology, Rolla, Missouri 65409, USA*
[3]*Institute of Nuclear Physics, Ulugbek, Tashkent 100214, Uzbekistan*

Differential studies of the proton-helium scattering problem using the two-center wave-packet convergent close-coupling approach is extended to the calculation of the ionization cross section differential in the electron emission energy and the projectile scattering angle. The results obtained using the correlated two-electron and effective one-electron methods are in reasonably good agreement with experiment. While the shape of the doubly differential cross section generally agrees with the results of the experiment, at some emission energies its magnitude does not. This appears consistent with similar disagreement seen in the singly differential cross section at the same emission energies.

I. INTRODUCTION

Studying simple four-body scattering problems, like that which is presented by collisions of protons with helium atoms, remains an important area of research. This is because these are fundamental systems with wide-ranging applications in areas such as astrophysics, plasma physics, and medical physics. Solving this problem in full remains a challenging theoretical problem. Progress has been made into probing elastic scattering, excitation, and electron-capture processes, however, few attempts have been made to investigate ionization in a nonperturbative manner [1–5]. For a recent review of energetic ion-atom and ion-molecule collisions, see Refs. [6–8].

The close-coupling formalism was first applied to proton-induced differential ionization of atomic hydrogen in Refs. [9,10]. Here, we consider single ionization of helium by proton impact in the intermediate energy region where the speed of the projectile is either comparable to or somewhat larger than the electron's orbital speed. At these energies coupling between various channels cannot be ignored. Modeling ionization is particularly challenging since the electron may be emitted into either the continuum of the target, hereafter called direct ionization (DI), or into the continuum of the projectile, called electron capture to the continuum (ECC). Therefore, two-center effects must be accounted for to accurately calculate ionization cross sections.

Higher-order effects have also been suggested to affect single-ionization cross sections. Measurements of the fully differential cross section for the ionization of helium in collisions with 75-keV protons by Schulz *et al.* [11] show peak structures when the projectile is scattered in the forward direction and the electron is emitted in the perpendicular direction. This may indicate some intricate two-electron mechanisms that are not well-studied. Furthermore, theory fails when it comes to describing two-electron processes like transfer excitation [12,13]. This indicates that the full proton-helium problem is far from being solved.

The doubly differential cross section (DDCS) for single ionization of helium as a function of projectile energy loss and scattering angle has been measured by Schulz *et al.* [14]. The corresponding theoretical calculations were reported in Refs. [14–18]. Due to the aforementioned difficulties in describing ionization, the theoretical approaches that have been employed are perturbational ones. Different implementations of the first Born approximation (FBA) with Hartree-Fock initial- and final-state wave functions were presented in Refs. [14–16,18]. Schulz *et al.* [14] and Dey and Roy [18] presented methods excluding and including the postcollision interaction, hereafter referred to as FBA and FBA-PCI, respectively. At 50 keV, the lowest projectile energy considered, none of the methods based on the first Born approximation agreed with the experimental data [14]. At higher projectile energies, however, agreement improved. The first Born approaches agreed with experimental data in the intermediate-angle region. For small angles, agreement was good when slow electrons were ejected but agreement worsened as ejected-electron energy increased. At large scattering angles, the Born approximation methods underestimated experimental data. At 300 keV, Salin [15] employed a modified FBA (denoted hereafter as FBA*) at various ejection energies; however, experimental measurements have not been conducted at this projectile energy. Godunov *et al.* [16] also implemented the second Born approximation at projectile energies of 50, 75, and 100 keV. For 50 keV, agreement is again poor but for 75 and 100 keV similar agreement was found in the small angle region and somewhat improved agreement for large angle scattering, although a discrepancy still persisted. Finally, Godunov *et al.* [16] presented a peaking approximation that gave fair agreement with the experiment [14] at 50 keV. However, the results were similar to the FBA ones at 75 and 100 keV.

_____
*kate.bain@postgrad.curtin.edu.au

The continuum-distorted-wave eikonal-initial-state (CDW-EIS) [17] theory is a perturbative method that was employed with greater success. Rodríguez and Barrachina [17] presented calculations for 50, 75, 100, and 150 keV. Good agreement was found at 75 and 100 keV across the angular range. At 50 keV, agreement was also good for the low ejected-electron energies but at the largest electron energy considered, the CDW-EIS method consistently underestimated the experimental data [14]. At all ejected-electron energies, agreement with experiment was achieved when the projectile is scattered into small angles but agreement was poor in the large-angle region at 150 keV. The Glauber approximation including (GA-PCI) and excluding the postcollision interaction was applied by Dey and Roy [18] for projectile energies of 50, 75, 100, and 150 keV. This method achieved better agreement for smaller projectile and ejected-electron energies but began to underestimate experimental results [14] at small and large angles as the electron ejection energy increased.

The classical-trajectory Monte Carlo (CTMC) approach was also employed by Schulz *et al.* [14] with moderate success. At the projectile energy of 50 keV, the CTMC was in very good agreement with the experiment [14] for the lowest ejected-electron energy presented, however, consistently underestimated it for the larger ejected-electron energies. At 100 and 150 keV though, only a few data points for this method were available. Agreement with the experiment of Schulz *et al.* [14] was better at 150 keV than at 100 keV.

Finally, a calculation based on the Faddeev-Merkuriev (FM) equations and using a simplified three-body model was presented by Godunov *et al.* [16] at 50, 75, and 100 keV. This method achieved fair agreement with the experimental data with results improving for larger ejected-electron energies.

Close-coupling approaches have certain challenges when calculating ionization cross sections related to the numerical evaluation of matrix elements and the modeling of the continuum, particularly in the energy range considered herein where the probability of capture into the continuum of the projectile cannot be ignored. The convergent close-coupling approach has been developed to circumvent the aforementioned difficulties through use of the fully quantum-mechanical [19,20], standard semiclassical [21], and wave-packet [10,22] implementations for the fundamental proton-hydrogen collision system. The wave-packet convergent close-coupling (WP-CCC) method has been extended to proton-helium differential ionization [23,24] at sufficiently high energies where electron-capture channels can be neglected. Also note that the integrated cross sections have been calculated using the two-center WP-CCC approach and the obtained results agree very well with experiment in a wide energy range including low, intermediate, and high energies [5].

Thus far, calculations of the singly differential cross sections (SDCS) using the two-center WP-CCC for binary processes have been completed and reported in Ref. [25] and all three types of singly differential ionization cross sections in Ref. [26]. It was concluded that the WP-CCC approach is capable of providing a complete, accurate, and detailed differential picture of the binary processes, as well as singly differential ionization, taking place in proton-helium collisions. In Ref. [27], the ionization cross section differential in the ejected-electron energy and angle was presented. In this work, the two-center four-body WP-CCC method is used to calculate the cross sections for ionization in proton-helium collisions doubly differential in the ejected-electron energy (which is equivalent to the energy loss by the projectile) and the projectile scattering angle at intermediate incident energies. For comparison, we also use a recently developed approach [28] that reduces the two-electron helium atom to an effective single-electron system convenient for scattering calculations.

Unless specified otherwise, atomic units (a.u.) are used throughout this paper.

II. TWO-CENTER WAVE-PACKET CONVERGENT CLOSE-COUPLING METHOD

Various aspects of the two-center wave-packet convergent close-coupling method for ion-atom collisions are described in detail in our earlier works [5,23,29,30]. The method has also been applied to proton collisions with molecular hydrogen [31–33]. A brief description of the method specific to doubly differential ionization is given in Ref. [27]. The cross section relevant to this paper is given below.

There are three types of doubly differential cross sections for ionization; the DDCS differential in the ejected-electron energy and angle, the DDCS differential in the electron ejection energy and projectile scattering angle, and, finally, the DDCS differential in the electron ejection angle and projectile scattering angle. The DDCS in ejected-electron energy and angle was presented in Ref. [27]. The DDCS for ionization differential in the scattering angle of the projectile and energy of the ejected electron can be calculated from the fully differential cross section as

$$\frac{d^2\sigma_{\text{ion}}}{dE_{\text{e}}d\Omega_f} = \int \frac{d^3\sigma_{\text{ion}}}{dE_{\text{e}}d\Omega_{\text{e}}d\Omega_f}d\Omega_{\text{e}}, \tag{1}$$

where Ω_{e} is the solid angle of $\boldsymbol{\kappa}$, the electron momentum in the laboratory frame, into which the electron is ejected, $E_{\text{e}} = \kappa^2/2$ is the ejected-electron energy, and Ω_f is the solid angle of the scattered projectile.

In the current two-center approach the fully differential cross section for ionization consists of the direct ionization and electron-capture into continuum components. It is important to note that the DI and ECC components of the cross sections do not represent a physical separation between the continuums of the projectile and the target. Rather they provide information on the dominant mechanisms at play in a particular kinematic regime. The DI and ECC amplitudes are written as the product of the projection of the positive-energy pseudostates on both centers onto the true Coulomb scattering wave function and the direct-scattering or electron-capture amplitudes, respectively. The direct-scattering and electron-capture amplitudes are, in turn, calculated from the impact-parameter space transition-probability amplitudes. For further details of the scattering amplitudes, see Refs. [25,26].

III. DOUBLY DIFFERENTIAL SINGLE-IONIZATION CROSS SECTION

Below we present the results obtained for the doubly differential cross section for proton-impact single-ionization
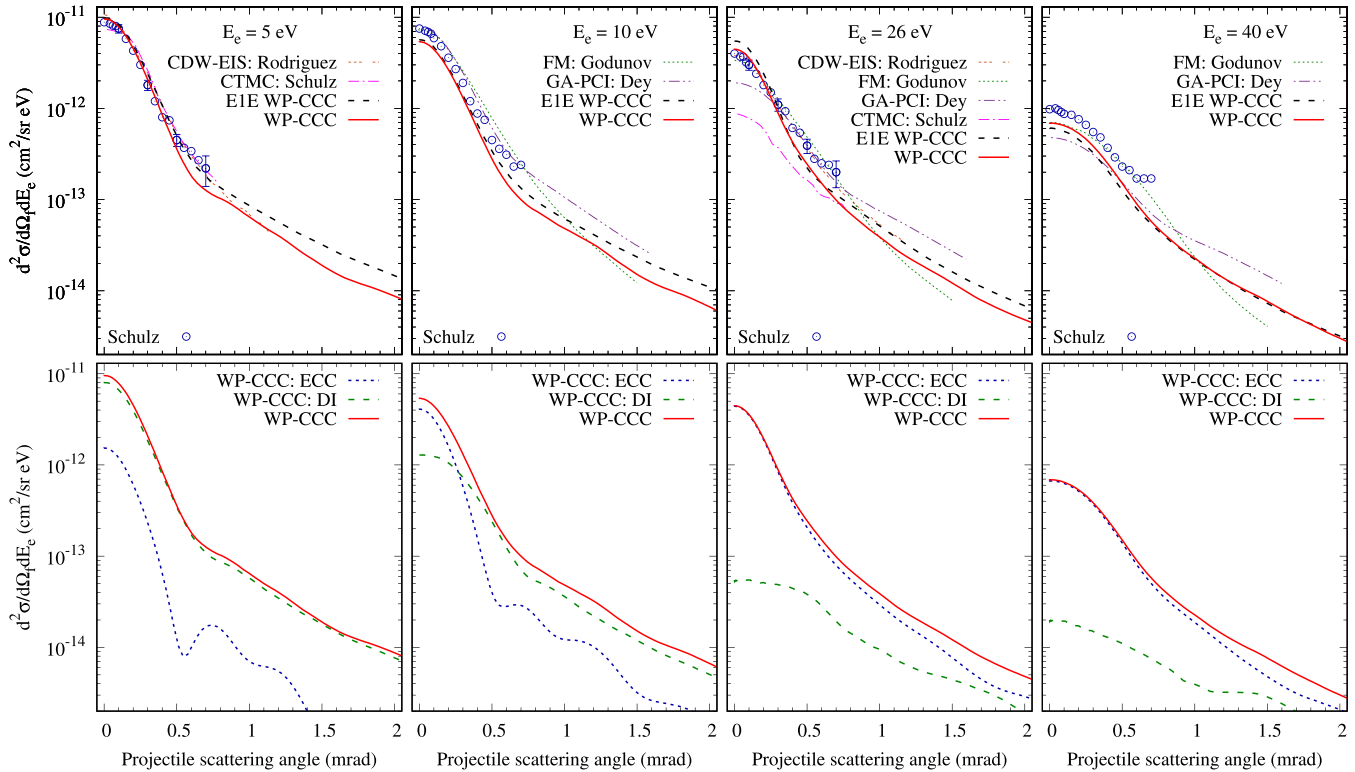
FIG. 1. Doubly differential cross section for single ionization of helium by 50 keV protons as a function of scattered-projectile angle. The ejected-electron energies are 5, 10, 26, and 40 eV. Experimental data are by Schulz *et al.* [14]. The solid line represents the present WP-CCC calculation. The long-dashed line represents the present E1E WP-CCC calculation. Other theoretical calculations are the CTMC of Schulz *et al.* [14], the CDW-EIS by Rodríguez and Barrachina [17], GA-PCI by Dey and Roy [18], and the FM by Godunov *et al.* [16].

of helium as a function of the projectile energy loss and scattering angle. To be consistent with our previous works, hereafter, instead of the projectile energy loss, we use the corresponding ejected-electron energy. The results calculated using Eq. (1) are presented at five intermediate incident energies: 50, 75, 100, 150, and 300 keV. The energies are given in the laboratory frame. As in Ref. [27], our main results obtained using the correlated two-electron wave-packet convergent close-coupling approach are denoted as WP-CCC. For comparison, we also present results obtained using the effective one-electron treatment of the helium target, hereafter denoted as E1E WP-CCC.

In both the two-electron and E1E WP-CCC approaches the number of included negative- and positive-energy pseudostates are increased until adequate convergence is achieved in the DDCS that we are interested in. Specifically, to achieve convergence in both approaches, a basis comprised of bound states up to principal quantum number 5 and 20 bin states for each orbital angular momentum was used on both centers at all incident projectile energies. The continuum was discretized up to a maximum electron momentum of 7 a.u. at 50 keV, 8 a.u. at 75 keV, and 10 a.u. at 100, 150, and 300 keV.

The impact parameters for all calculations ranged from 0 to 40 a.u., which was found to be sufficient for the probability of all collision processes to fall off several orders of magnitude. Finally, in all cases, the expansion coefficients representing the transition amplitudes were solved on a grid ranging from −200 a.u. to +200 a.u. for all impact parameters. For

convergence of the total DDCS, 600 points were sufficient, however, for the components to converge separately, 1000 points were required.

The FBA-PCI approach was employed by Schulz *et al.* [14] and Dey and Roy [18] for projectile energies of 50, 75, 100, and 150 keV at various electron ejection energies, however, the results were in poor agreement with experimental data. For clarity in the corresponding figures, these results are not included.

Energy distribution of ejected electrons as a function of projectile angle

Results obtained for a proton-impact energy of 50 keV within the two-electron WP-CCC approach are presented in Fig. 1 in comparison with the present E1E results, experimental data [14], and other calculations [14,16–18]. In the lower panels, the DI and ECC components of the DDCS obtained within the two-electron WP-CCC method are shown.

At an ejection energy of 5 eV, the WP-CCC results are in good agreement with the data, slightly underestimating the last few experimental points when the projectile is scattered into angles above 0.5 mrad. The E1E WP-CCC results coincide with the WP-CCC ones in the forward cone but begin to deviate around 0.5 mrad. The two methods maintain the same shape but, above 0.5 mrad, the E1E WP-CCC results lie above the two-electron WP-CCC ones which, somewhat surprisingly, brings the E1E WP-CCC results into better agreement with the experiment for the final points. The CDW-EIS results
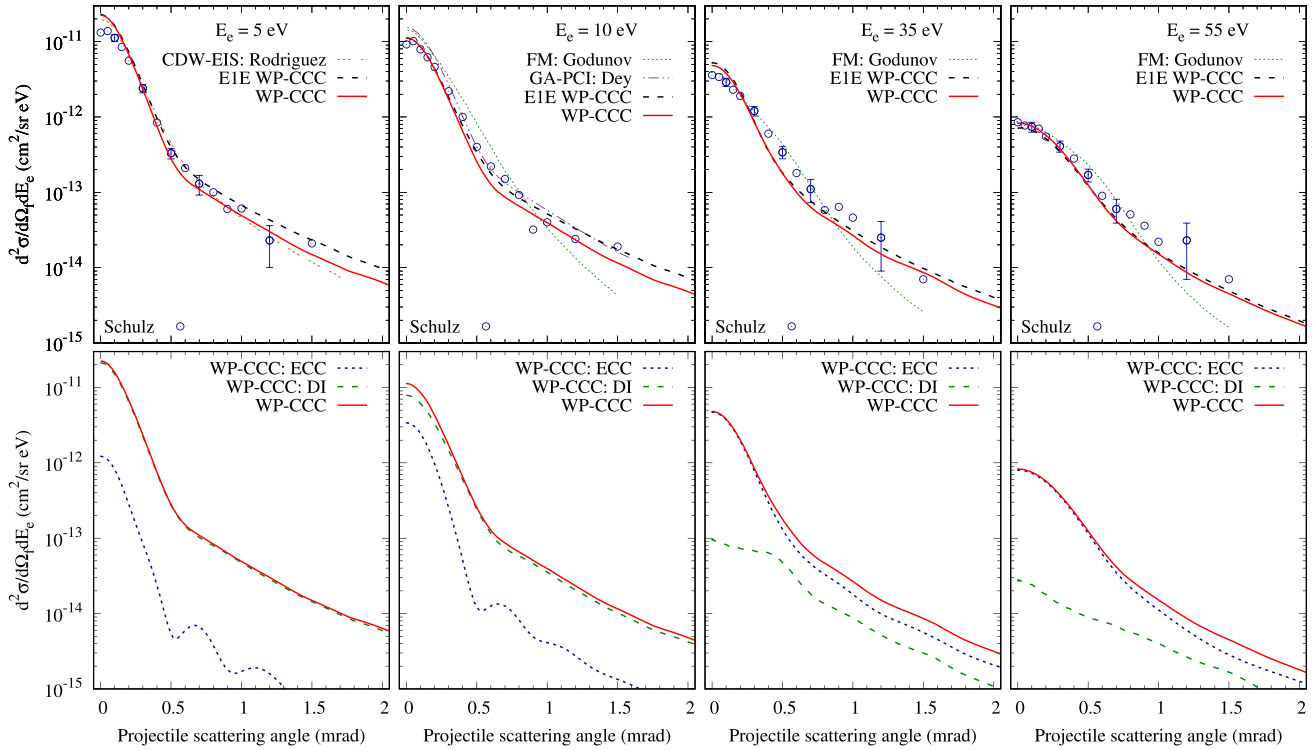
FIG. 2. Doubly differential cross section for ionization of helium by 75 keV protons as a function of scattered-projectile angle. The electron is ejected at energies of 5, 10, 35, and 55 eV. Experimental data are by Schulz *et al.* [14]. The solid line represents the present WP-CCC calculation. The long-dashed line represents the present E1E WP-CCC calculation. Other theoretical calculations are the CDW-EIS by Rodríguez and Barrachina [17], GA-PCI by Dey and Roy [18], and the FM by Godunov *et al.* [16].

by Rodríguez and Barrachina [17] align very well with the E1E WP-CCC ones in the region where the experiment is available. Past this point, at around 0.7 mrad, the CDW-EIS results continue to fall rapidly whereas the WP-CCC ones fall off more slowly due to the heavy-particle interaction being included. The CTMC results of Schulz *et al.* [14], available up to 0.8 mrad, also practically coincide with the E1E WP-CCC ones except in the forward-scattering region where the CTMC method underestimates the experiment and all other theoretical calculations.

The results of the WP-CCC approaches at 10 eV again agree with each other very well up to 0.5 mrad. For larger scattering angles, the two-electron WP-CCC results fall below the E1E WP-CCC ones. Both are in fair agreement with the experiment. The FM method of Godunov *et al.* [16] and GA-PCI by Dey and Roy [18] consistently overestimate the experimental data up to 0.7 mrad. After 0.7 mrad, the FM and GA-PCI results deviate as the FM ones continue to fall while the GA-PCI results fall off more slowly, similar to the E1E and two-electron WP-CCC ones.

The ejected-electron energy of 26 eV is closest to the velocity matching point of 27.2 eV. Our results from both WP-CCC methods for this ejection energy agree with the experimental data very well for scattering angles below 0.5 mrad, however, predict a slightly steeper falloff for larger angles.[1] The deviation of the two methods at the larger scat-

tering angles is reduced with the E1E WP-CCC method again leading to slightly larger DDCS. The results of the CDW-EIS approach [17] agree well with the experiment at this emission energy in the entire angular region where measurements were taken. The shape of these results also matches well with that of our DDCS. The FM method by Godunov *et al.* [16] also agrees with experiment though again their DDCS falls off after 0.5 mrad faster than the other ones. The GA-PCI approach [18] underestimates the experiment for scattering angles less than 0.3 mrad but is in good agreement elsewhere. The GA-PCI results also match the E1E WP-CCC and WP-CCC ones in terms of shape. The CTMC results underestimate the experimental measurements.

At an ejection energy of 40 eV, the results of our E1E and two-electron WP-CCC approaches practically coincide at all scattering angles but consistently underestimate the experiment. The GA-PCI [18] results also do not agree well with the data. While the results produced by the FM method [16] do pass through a few experimental points around 0.5 mrad, they also do not agree overall. The magnitude of the DDCS at 0 mrad is very close to that obtained in our methods, meaning that it also underestimates the experiment. Furthermore, the shape of the DDCS obtained in the FM approach does not match that of the other theoretical calculations nor is it supported by experimental data.

In the bottom panel, the DI and ECC components of the DDCS obtained in the WP-CCC method are presented. It is seen that the ECC component dominates at and above the matching velocity but is negligible at the smallest electron energy. The DI component, on the other hand, dominates the

---

[1]Note that there is a misprint in Fig. 3 of Ref. [14]. The electron energy should read 26 eV.
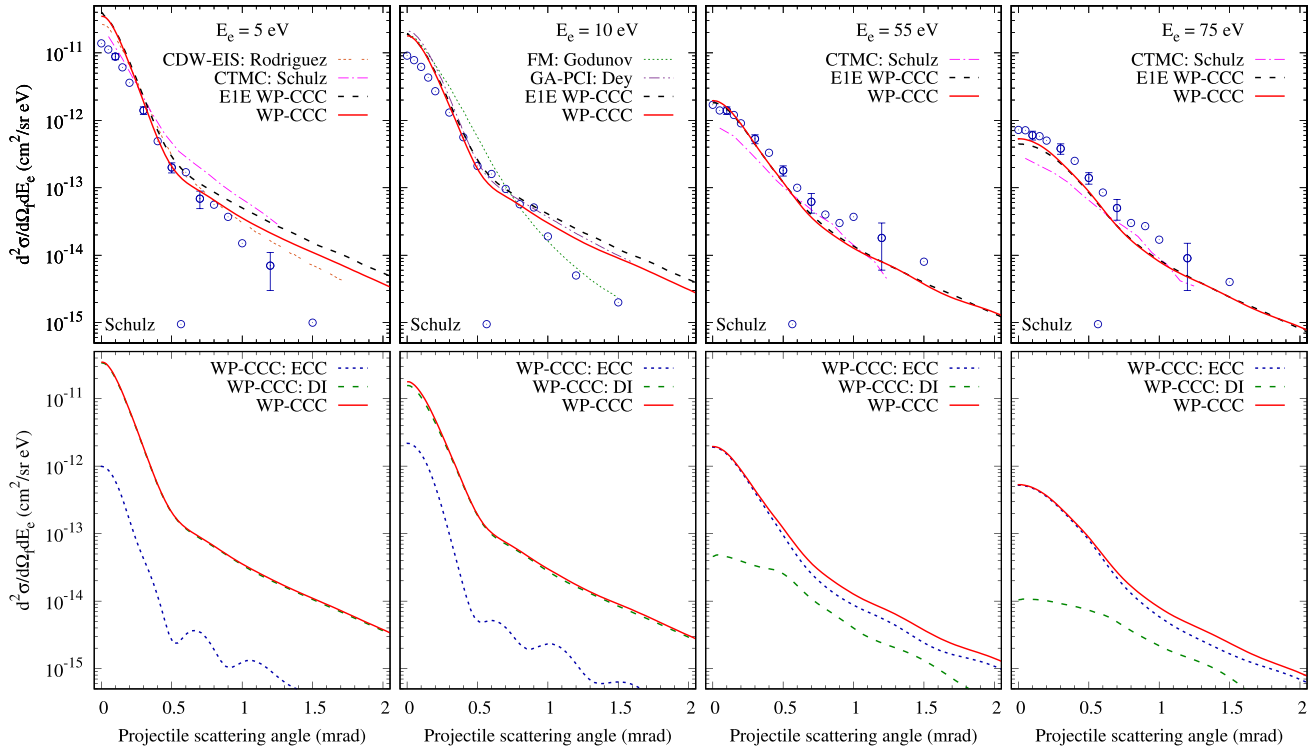
FIG. 3. Doubly differential cross section for ionization of helium by 100 keV protons as a function of scattered-projectile angle. The electron is ejected with energies of 5, 10, 55, and 75 eV. Experimental data by Schulz *et al.* [14]. The solid line represents the present WP-CCC calculation. The long-dashed line represents the present E1E WP-CCC calculation. Other theoretical calculations are the CTMC of Schulz *et al.* [14], the CDW-EIS by Rodríguez and Barrachina [17], GA-PCI by Dey and Roy [18], and the FM by Godunov *et al.* [16].

DDCS when the ejected electrons are slow and is negligible at large electron energies. It is also interesting to note that the ECC cross section becomes larger as it nears the matching velocity for small scattering angles. Also, at the 5 and 10 eV ejection energies, we see oscillations in the ECC cross section. This feature does not appear in the ECC DDCS obtained in the E1E WP-CCC method (not shown in the figure) which indicates that it could be a manifestation of the complex two-electron structure. These oscillations are not present for larger electron ejection energies either.

The results obtained for a projectile energy of 75 keV are presented in Fig. 2 in comparison with experimental data as well as other calculations [14,16–18]. Agreement between the results of the WP-CCC and E1E WP-CCC methods and the experiment is very good at an electron ejection energy of 5 eV. Near the forward-scattering direction, the DDCS obtained within the WP-CCC approaches coincide with each other but slightly overestimate the experiment. Beyond 0.3 mrad, the two-electron and E1E WP-CCC results deviate with the E1E WP-CCC ones being larger. Within the experimental uncertainty, results from both methods are still in agreement with the data. The CDW-EIS results [17] also agree well with both the WP-CCC ones and experimental measurements. The CDW-EIS results align with the E1E WP-CCC ones up to 0.6 mrad. However, beyond 0.6 mrad, they fall at a faster rate.

The situation with the results from both WP-CCC methods is much the same for a 10 eV emission energy. In close alignment with the E1E WP-CCC results are those produced by the GA-PCI method [18]. The results from the FM calculation by

Godunov *et al.* [16] disagree with experimental data at large scattering angles. At 0 mrad, the magnitude is similar to that of the WP-CCC results, however, the FM ones tend to fall at a constant rate after this peak so that they overestimate the experiment for angles below 0.8 mrad, then underestimate it at larger angles.

For an ejected-electron energy of 35 eV, the energy closest to the velocity matching point of 40.8 eV at 75 keV projectile energy, the WP-CCC cross sections again agree well in terms of magnitude but fall more quickly than the experimental data. Our results, however, appear to be within the experimental uncertainty at least around 1.2 mrad. At an electron ejection energy of 55 eV, the picture is quite similar except the DDCS obtained within the two-electron WP-CCC method is in excellent agreement with experimental data in the forward direction.

The comparison between the DI and ECC channels is similar to 50 keV. The lower panels show that for 5 eV, the DI component is an order of magnitude larger than that of the ECC. At 10 eV, DI is still the dominant channel but, as at a collision energy of 50 keV, the ECC DDCS reaches its peak. ECC then becomes the dominant channel for 35 and 55 eV as the DI component continues to diminish. Again, the oscillations for the 5 and 10 eV ejection energy cross sections appear in the ECC component.

The upper panels in Fig. 3 show the present results for a proton energy of 100 keV obtained using the two-electron and E1E WP-CCC methods in comparison with experimental data and other calculations [14,16–18]. At an electron ejection energy of 5 eV, the WP-CCC results again overestimate
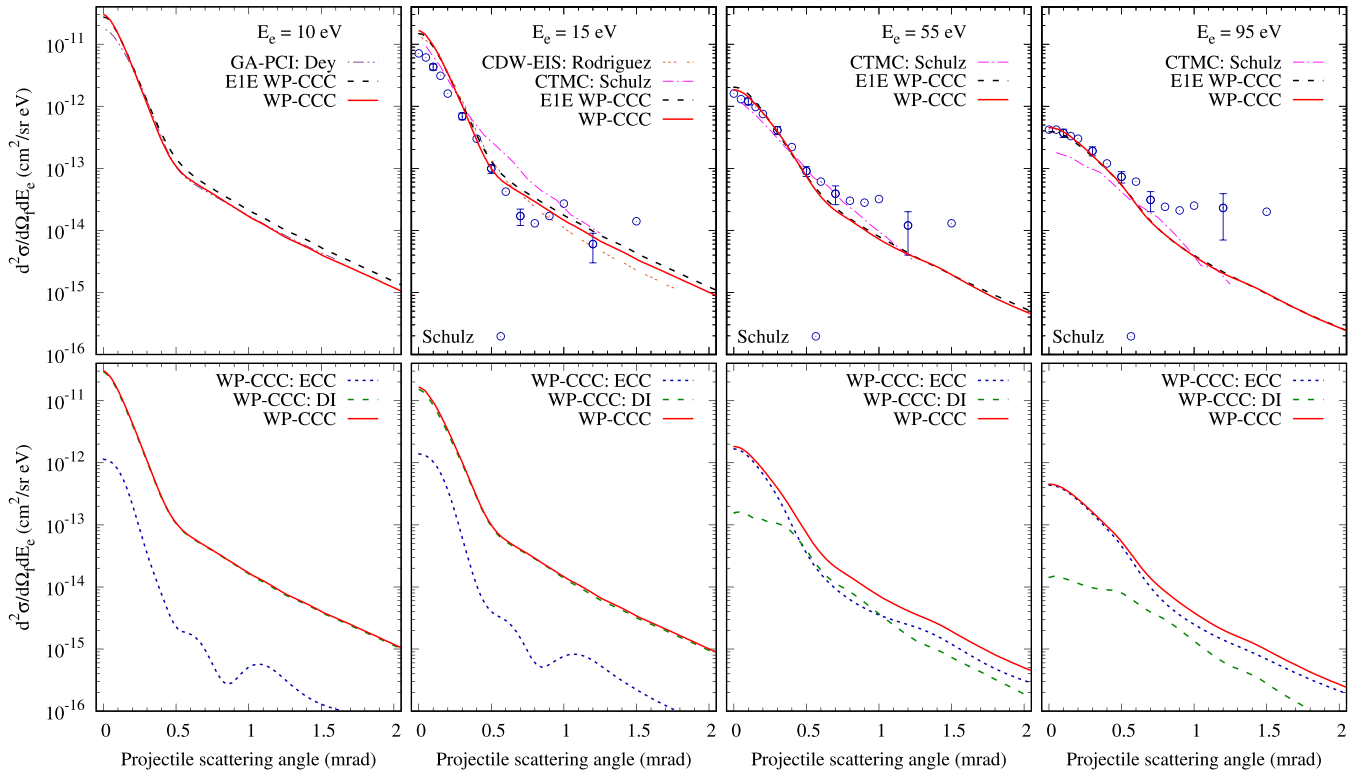
FIG. 4. Doubly differential cross section for ionization of helium by 150 keV protons as a function of scattered-projectile angle. The electron is ejected at energies of 10, 15, 55, and 95 eV. Experimental data are by Schulz *et al.* [14]. The solid line represents the present WP-CCC calculation. The long-dashed line represents the present E1E WP-CCC calculation. Other theoretical calculations are the GA-PCI by Dey and Roy [18], the CTMC by Schulz *et al.* [14], and the CDW-EIS by Rodríguez and Barrachina [17].

the experiment in the narrow forward-scattering direction but show very good agreement in the intermediate angle region only to overestimate the final few experimental points. The E1E WP-CCC results agree fairly well with the fully correlated calculation, although, due to the deviation from the WP-CCC ones above 0.5 mrad, tends to slightly overestimate the experiment. The comparison between our calculations and CDW-EIS [17] ones is quite similar to 75 keV. Agreement with the WP-CCC results is good up to 1 mrad. After 1 mrad, the CDW-EIS results begin to fall at a faster rate, however, this does not bring them into agreement with experiment. The CTMC results [14] are too large everywhere that the calculation was performed though do reproduce the shape of the experiment quite well. The situation at 10 eV is similar as far as the WP-CCC and E1E WP-CCC results are concerned. The GA-PCI [18] results also show moderate agreement with the experiment. The results from the FM approach by Godunov *et al.* [16] have the same magnitude as the GA-PCI and WP-CCC ones around 0 mrad but achieve agreement with the last three experimental points as well. At 55 eV, the electron energy nearest the velocity matching point of 54.4 eV, and 75 eV, the two-electron and E1E WP-CCC DDCS practically coincide. The results agree very well with the experimental data [14]. At 75 eV, however, the WP-CCC cross sections slightly underestimate it. The error bar shown for large-angle scattering indicates that our calculations are within the experimental uncertainty in this region. The CTMC method by Schulz *et al.* [14] is unsuccessful in terms of both shape and magnitude. The bottom panels show that the relative

importance of the DI and ECC components of the DDCS is the same as at 50 and 75 keV.

At the projectile energy of 150 keV, the results obtained within the two-electron WP-CCC approach and the E1E WP-CCC approach are presented in Fig. 4 in comparison with experimental data and other calculations [14,16–18]. There are no experiments for comparison at an electron ejection energy of 10 eV. At this energy the two-electron and E1E WP-CCC results only slightly diverge past 0.5 mrad. The GA-PCI [18] data is in excellent agreement with the WP-CCC ones. For electrons ejected with an energy of 15 eV, the present WP-CCC data overestimates the forward direction. However, from 0.3 mrad, the results are in good agreement with the general trend of the experimental data. The CDW-EIS [17] results also show good agreement with the experiment. The CTMC results of Schulz *et al.* [14] align with all other theoretical treatments for the forward peak though disagree with these theories and the experiment everywhere else. The forward-scattering peak is reproduced very well by the E1E and two-electron WP-CCC data at 55 eV. At scattering angles greater than 0.5 mrad, the WP-CCC results begin to underestimate the experiment. The CTMC method applied by Schulz *et al.* [14] does not agree well with the experimental data except near 0 mrad. The results obtained by the WP-CCC and E1E WP-CCC approaches are in perfect agreement with one another at an electron ejection energy of 95 eV. The results are in excellent agreement with the experiment near the forward peak. Beyond 0.5 mrad, the experiment appears to be flat whereas our calculations continue to fall. The CTMC results [14] again disagree
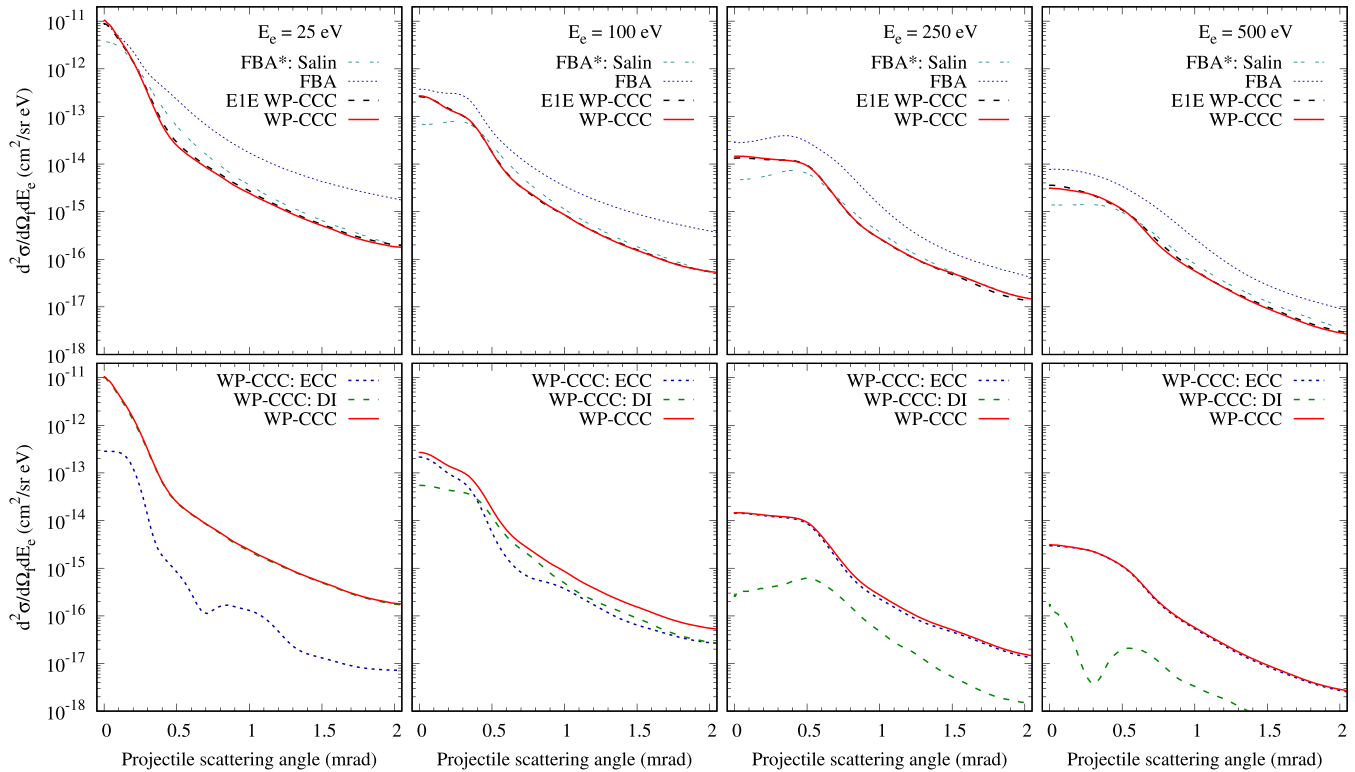
FIG. 5. Doubly differential cross section for ionization of helium by 300 keV protons as a function of scattered-projectile angle. The electron is ejected at energies of 25, 100, 250, and 500 eV. The solid line represents the present WP-CCC calculation. The long-dashed line represents the present E1E WP-CCC calculation. The short-dashed line is the present FBA calculation. The other theoretical calculation is the FBA* of Salin [15].

with our data and the experimental data. For this projectile energy, the velocity matching point is 81.7 eV, so 95 eV is the closest electron energy considered in the experiment [14]. The lower panels show that the breakup of the DDCS is similar to lower projectile energies considered here.

We note that, in the same publication, Schulz *et al.* [14] also presented the singly differential cross section of ionization as a function of ejected-electron energy. This SDCS was calculated using the WP-CCC approach in Ref. [26]. At 75 and 100 keV, agreement with the SDCS was generally good, which is reflected in the present DDCS. The SDCS at 150 keV, however, did not agree well with the SDCS calculated within the WP-CCC method. At small ejection energies, our results overestimated the experimental SDCS as can be seen in the 15 eV panel in Fig. 4. The energy of 55 eV, where the DDCS presented here agrees fairly well, corresponds to the point in the SDCS where the experiment and our WP-CCC calculation cross. At larger ejection energies, our SDCS underestimated the experiment which is also reflected in the 95 eV panel of this calculation.

Finally, the results obtained within the two-electron and E1E WP-CCC approaches at the projectile energy of 300 keV are presented in the upper panels of Fig. 5 in comparison with the calculation of Salin [15] and the present FBA ones. No experiments are available at this projectile energy. At all four electron ejection energies considered here, the DDCS from two-electron WP-CCC and E1E WP-CCC methods practically coincide, possibly indicating that the projectile is energetic enough to become less sensitive to electron-electron

correlation effects. The FBA* results of Salin [15] are obtained by introducing a phase factor depending on the heavy-particle interaction, which indeed somewhat reduces the FBA. The FBA* results generally agree well with our calculations except for scattering into angles less than 0.5 mrad. In this region, the FBA* results tend to underestimate the WP-CCC ones. There is a peak seen at around 0.5 mrad in the FBA and FBA* calculations at 100, 250, and 500 eV. Within the WP-CCC approaches, this corresponding peak in the DDCS is more identifiable in the ECC component shown in the bottom panel. This structure could be explained by the electron being ejected in the region of the projectile producing the binary-encounter peak possibly via Thomas double scattering. The Thomas mechanism typically results in a strong peak near 0.5 mrad for fast projectiles, however, at 300 keV its influence is weak but visible in this DDCS. The bottom panel shows that DI is by far the dominant channel for ejection of slow electrons. At 100 eV, DI and ECC are comparable and the ECC cross section is the largest of all the ejection energies. At 250 and 500 eV, the ECC channel dominates by approximately an order of magnitude. At the lowest ejection energy, 25 eV, the oscillations due to helium structure are much less prominent.

In summary, the results obtained from the E1E and two-electron WP-CCC approaches presented in Figs. 1–4 are in fair agreement with the experimental data by Schulz *et al.* [14] for the DDCS differential in the ejected-electron energy and scattered projectile angle. Furthermore, the simpler E1E WP-CCC method produces data that agree very well with

those from the fully correlated two-electron WP-CCC method.

IV. CONCLUSION

Differential ionization in proton-helium collisions is investigated using the two-center wave-packet convergent close-coupling method. The study is performed in a non-perturbative manner in the intermediate-energy region where coupling between various channels cannot be ignored. For these projectile energies, the probability of electron capture into the continuum of the projectile is comparable to that of ionization into the target continuum. Hence, a two-center approach is required for accuracy when calculating cross sections. These challenges, particularly when investigating differential ionization, preclude many theories from performing calculations. It is well known that the sophisticated coupled-channel approaches to ion-atom collisions that can give good results for the integrated ionization cross section cannot be applied to differential ionization. The reason for this is that these methods do not give information on the ionization amplitude required for the differential cross sections, at least at this stage. On the other hand, the WP-CCC method is based on calculating the ionization amplitude. The approach uses a correlated two-electron wave function for the helium target and discretizes the continuum using wave-packet pseudostates. A simpler version of the WP-CCC reduces the target to an effective single-electron system.

The energy distribution of ejected electrons as a function of scattered projectile angle is calculated. The direct ionization and electron capture to the continuum components of the doubly differential cross section are also presented. This provides previously unseen insight into the dominant mechanisms at play in different kinematic regimes. Results from the two WP-CCC methods agree very well with each other. This finding suggests that the simpler E1E approach is also able to provide insight into the physics of the present doubly differential ionization cross section. The obtained results are compared with the only available experiment by Schulz et al. [14]. Agreement is generally good but depends on all three parameters: incident energy, scattering angle, and ejected-electron energy. This is not an unexpected outcome as, in Ref. [26], we compared with

the singly differential ionization cross section as a function of emitted-electron energy presented by Schulz et al. [14] with similarly varied agreement. The DDCS in energy and angle of the electron presented in Ref. [27] also agreed very well with the available experiments. Furthermore, the total ionization cross sections presented in Ref. [5] are in perfect agreement with experimental data. Agreement with the integrated and other differential ionization cross sections from a single calculation supports the DDCS presented here. Analysis provided in previous works, see Refs. [25–27], regarding intermediate energy proton-helium collisions demonstrates that the WP-CCC method is a unique approach capable of providing a realistic and accurate differential picture of this system. The results presented in this work demonstrate the potential of the WP-CCC method to investigate the helium ionization process further and calculate the fully differential cross section. Fully differential ionization of helium by ion impact remains one of the most challenging problems in atomic collision physics. There is a discrepancy between theory and the experimental data by Schulz et al. [11] at the intermediate projectile energy of 75 keV. The WP-CCC approach may be able to help better understand the situation.

Establishing a record of consistent, reliable and accurate integrated, singly and doubly differential cross sections is imperative in this effort. Our ultimate goal is to solve the proton-helium ionization problem in a kinematically complete fashion. We also plan to investigate if higher-order effects, that have not previously been considered within the WP-CCC method, are influencing high-energy proton-helium ionization cross sections [34] and C^{6+}-helium ionization cross sections [35].

[1] H. A. Slim, E. L. Heck, B. H. Bransden, and D. R. Flower, J. Phys. B: At., Mol. Opt. Phys. **24**, L421 (1991).

[2] T. G. Winter, Phys. Rev. A **44**, 4353 (1991).

[3] M. Baxter and T. Kirchner, Phys. Rev. A **93**, 012502 (2016).

[4] J. W. Gao, T. Miteva, Y. Wu, J. G. Wang, A. Dubois, and N. Sisourat, Phys. Rev. A **103**, L030803 (2021).

[5] S. U. Alladustov, I. B. Abdurakhmanov, A. S. Kadyrov, I. Bray, and K. Bartschat, Phys. Rev. A **99**, 052706 (2019).

[6] M. Pindzola, J. Colgan, F. Robicheaux, T. Lee, M. Ciappina, M. Foster, J. Ludlow, and S. Abdel-Naby in *Time-Dependent Close-Coupling Calculations for Ion-Impact Ionization of Atoms and Molecules*, edited by E. Arimondo, C. C. Lin, and S. F. Yelin (Academic Press, 2016), pp. 291–319.

[7] *State-of-the-Art Reviews on Energetic Ion-Atom and Ion-Molecule Collisions*, edited by D. Belkić, I. Bray, and A. Kadyrov (World Scientific, Singapore, 2019).

[8] *Ion-Atom Collisions: The Few-Body Problem in Dynamic Systems*, edited by M. Schulz (De Gruyter, Berlin, Boston, 2019).

[9] H. R. J. Walters and C. T. Whelan, Phys. Rev. A **92**, 062712 (2015).

[10] I. B. Abdurakhmanov, J. J. Bailey, A. S. Kadyrov, and I. Bray, Phys. Rev. A **97**, 032707 (2018).

[11] M. Schulz, A. Hasan, N. V. Maydanyuk, M. Foster, B. Took, and D. H. Madison, Phys. Rev. A **73**, 062704 (2006).

[12] A. Hasan, B. Tooke, M. Zapukhlyak, T. Kirchner, and M. Schulz, Phys. Rev. A **74**, 032703 (2006).

[13] M. S. Schöffler, H.-K. Kim, O. Chuluunbaatar, S. Houamer, A. G. Galstyan, J. N. Titze, T. Jahnke, L. P. H. Schmidt, H. Schmidt-Böcking, R. Dörner, Y. V. Popov, and A. A. Bulychev, Phys. Rev. A **89**, 032707 (2014).

[14] M. Schulz, T. Vajnai, A. D. Gaus, W. Htwe, D. H. Madison, and R. E. Olson, Phys. Rev. A **54**, 2951 (1996).

[15] A. Salin, J. Phys. B: At., Mol. Opt. Phys. **22**, 3901 (1989).

[16] A. L. Godunov, V. A. Schipakov, and M. Schulz, J. Phys. B: At., Mol. Opt. Phys. **31**, 4943 (1998).

[17] V. D. Rodríguez and R. O. Barrachina, Phys. Rev. A **57**, 215 (1998).

[18] R. Dey and A. Roy, Nucl. Instrum. Methods Phys. Res., Sect. B **225**, 207 (2004).

[19] I. B. Abdurakhmanov, A. S. Kadyrov, S. K. Avazbaev, and I. Bray, J. Phys. B: At., Mol. Opt. Phys. **49**, 115203 (2016).

[20] I. B. Abdurakhmanov, A. S. Kadyrov, and I. Bray, J. Phys. B: At., Mol. Opt. Phys. **49**, 03LT01 (2016).

[21] S. K. Avazbaev, A. S. Kadyrov, I. B. Abdurakhmanov, D. V. Fursa, and I. Bray, Phys. Rev. A **93**, 022710 (2016).

[22] I. B. Abdurakhmanov, A. S. Kadyrov, and I. Bray, Phys. Rev. A **94**, 022703 (2016).

[23] I. B. Abdurakhmanov, A. S. Kadyrov, I. Bray, and K. Bartschat, Phys. Rev. A **96**, 022702 (2017).

[24] I. B. Abdurakhmanov, A. S. Kadyrov, S. U. Alladustov, I. Bray, and K. Bartschat, Phys. Rev. A **100**, 062708 (2019).

[25] K. H. Spicer, C. T. Plowman, I. B. Abdurakhmanov, A. S. Kadyrov, I. Bray, and S. U. Alladustov, Phys. Rev. A **104**, 032818 (2021).

[26] K. H. Spicer, C. T. Plowman, I. B. Abdurakhmanov, S. U. Alladustov, I. Bray, and A. S. Kadyrov, Phys. Rev. A **104**, 052815 (2021).

[27] K. H. Spicer, C. T. Plowman, S. U. Alladustov, I. B. Abdurakhmanov, I. Bray, and A. S. Kadyrov, Eur. Phys. J. D **77**, 131 (2023).

[28] I. B. Abdurakhmanov, C. T. Plowman, K. H. Spicer, I. Bray, and A. S. Kadyrov, Phys. Rev. A **104**, 042820 (2021).

[29] I. Abdurakhmanov, O. Erkilic, A. Kadyrov, I. Bray, S. Avazbaev, and A. Mukhamedzhanov, J. Phys. B: At., Mol. Opt. Phys. **52**, 105701 (2019).

[30] I. B. Abdurakhmanov, S. U. Alladustov, J. J. Bailey, A. S. Kadyrov, and I. Bray, Plasma Phys. Control. Fusion **60**, 095009 (2018).

[31] C. T. Plowman, I. B. Abdurakhmanov, I. Bray, and A. S. Kadyrov, Eur. Phys. J. D **76**, 31 (2022).

[32] C. T. Plowman, I. B. Abdurakhmanov, I. Bray, and A. S. Kadyrov, Eur. Phys. J. D **76**, 129 (2022).

[33] C. T. Plowman, I. B. Abdurakhmanov, I. Bray, and A. S. Kadyrov, Phys. Rev. A **107**, 032824 (2023).

[34] O. Chuluunbaatar, K. A. Kouzakov, S. A. Zaytsev, A. S. Zaytsev, V. L. Shablov, Y. V. Popov, H. Gassert, M. Waitz, H.-K. Kim, T. Bauer, A. Laucke, C. Müller, J. Voigtsberger, M. Weller, J. Rist, K. Pahl, M. Honig, M. Pitzer, S. Zeller, T. Jahnke *et al.*, Phys. Rev. A **99**, 062711 (2019).

[35] M. Schulz, R. Moshammer, D. Fischer, H. Kollmus, D. H. Madison, S. Jones, and J. Ullrich, Nature (London) **422**, 48 (2003).